

Minerva Access is the Institutional Repository of The University of Melbourne

Author/s:

Liu, H;Francis, L;Dagley, LF;Cobbold, SA;Webb, AI;Komander, D;Villadangos, JA;Mintern, JD

Title:

Major histocompatibility class II in murine antigen presenting cells is modified with a branched K63 and K11-linked ubiquitin chain

Date:

2025

Citation:

Liu, H., Francis, L., Dagley, L. F., Cobbold, S. A., Webb, A. I., Komander, D., Villadangos, J. A. & Mintern, J. D. (2025). Major histocompatibility class II in murine antigen presenting cells is modified with a branched K63 and K11-linked ubiquitin chain. *Scientific Reports*, 15 (1), <https://doi.org/10.1038/s41598-025-25817-4>.

Persistent Link:

<https://hdl.handle.net/11343/367966>

License:

CC BY-NC-ND



OPEN Major histocompatibility class II in murine antigen presenting cells is modified with a branched K63 and K11-linked ubiquitin chain

Haiyin Liu¹, Lauren Francis¹, Laura F. Dagley^{2,3}, Simon A. Cobbold^{3,4}, Andrew I. Webb^{2,3}, David Komander^{3,4}, Jose A. Villadangos^{1,5}✉ & Justine D. Mintern¹✉

Major histocompatibility class II (MHC II) is critical for adaptive immunity. MHC II intracellular trafficking and degradation is regulated by ubiquitination. Poly-ubiquitination (Ub) of MHC II directs it away from the plasma membrane and is a critical determinant of MHC II turnover. The MHC II Ub chain has not been characterized. Here, we describe the poly-Ub chain associated with MHC II in primary murine antigen presenting cells; conventional dendritic cells (cDCs) and B cells. Analysis was conducted for endogenous murine MHC II isoforms H2-A and H2-E immunoprecipitated from primary cells. We show that ubiquitination of both I-A and I-E expressed by cDCs and B cells is dependent on the E3 Ub ligase MARCH1. Using mass spectrometry Ub chain linkage analysis and innovative Ub “clipping” proteomics we comprehensively defined the features of the MHC II poly-Ub chain. This revealed the MARCH1-dependent poly-Ub chain associated with MHC II is composed of a branched chain with K11 and K63 Ub chain linkages. This is the first description of the Ub chain linkages and architecture associated with MARCH1-mediated ubiquitination of MHC II in primary antigen presenting cells. This is important because it creates possibilities for manipulation of MHC II function in adaptive immunity.

Ubiquitination represents a complex post-translational regulatory system, whereby ubiquitin (Ub), an 8.5 kDa protein, tags proteins to dictate their traffic, fate and function¹. Conjugation of Ub involves a three-step reaction mediated by E1, E2 and E3 Ub ligases. The resulting modification is highly dynamic, with established poly-Ub chains being edited or cleaved by deubiquitinating enzymes (DUBs). Poly-Ub chains form when Ub attached to a substrate serves as a substrate for additional rounds of ubiquitination. Any of the seven conserved internal Ub lysine residues (K6, K11, K27, K29, K33, K48 and K63), in addition to the N-terminal α -amino group, of the acceptor Ub can serve as binding sites, resulting in poly-Ub chains of varying lengths and architecture. Ub modifications are collectively known as the *Ub-code*¹. Ub codes act as versatile signals for downstream processing of the ubiquitinated substrate. For example, transmembrane proteins are predominantly associated with K63-, and in some cases, K11-linked poly-Ub chains that act as tags that direct their intracellular transport. K63-linked poly Ub chains are recognized by endosomal complexes required for transport and promote lysosomal protein degradation. In addition to homotypic chains, where all Ub chain linkages are the same, heterotypic and branched Ub chains made from combinations of different Ub chain linkages have also been identified, but their specific biological functions are largely uncharacterized^{2,3}.

Major histocompatibility complex (MHC) class II is a key component of the adaptive immune system. Its traffic to and from the plasma membrane is regulated by ubiquitination. In hemopoietic antigen presenting cells, MHC II is ubiquitinated by the E3 Ub ligase membrane associated RING-CH 1 (MARCH1)⁴. MARCH8, a closely related family member, performs this function in epithelial antigen presenting cells⁵⁻⁷. Ubiquitination of MHC II and its regulation of MHC II intracellular trafficking has important consequences for many aspects of adaptive immunity⁸. These include complement component C3 turnover and B cell-mediated conventional

¹Department of Biochemistry and Pharmacology, Bio21 Molecular Science and Biotechnology Institute, The University of Melbourne, 30 Flemington Rd, Parkville, VIC 3010, Australia. ²Advanced Technology and Biology Division, The Walter and Eliza Hall Institute of Medical Research, Parkville, VIC 3010, Australia. ³Department of Medical Biology, University of Melbourne, Melbourne, VIC 3052, Australia. ⁴Ubiquitin Signaling Division, The Walter and Eliza Hall Institute of Medical Research, Parkville, VIC 3010, Australia. ⁵Department of Microbiology and Immunology, Peter Doherty Institute for Infection and Immunity, The University of Melbourne, Parkville, VIC 3010, Australia. ✉email: j.villadangos@unimelb.edu.au; jmintern@unimelb.edu.au

dendritic cell (cDC) trogocytosis⁷, germinal center B cell responses⁹, antigen presentation and dendritic cell (DC) function^{10–15}, regulatory T cell development^{16,17}, and CD4⁺ T cell immunity¹⁸. Despite the importance of MHC II in immune responses, the MHC II-associated Ub code has yet to be characterized in primary immune cells. The Ub chain architecture and topology of the Ub chain associated with MHC II is unknown. Knowledge of the Ub code associated with MHC II is important to gain insight into the molecular mechanisms by which this critical immune protein is regulated.

In addition, the specific Ub chains generated by MARCH E3 Ub ligases have not been previously described. This is important because MARCH enzymes play important roles not only in MHC II ubiquitination, but in the ubiquitination of transmembrane proteins that participate in host anti-pathogen defense, cancer, diabetes and asthma⁸.

Here, we have investigated, and characterized in detail, MHC II ubiquitination in primary antigen presenting cells, namely cDCs and B cells. Analysis of the MARCH1 mediated MHC II Ub “code” in primary immune cells identifies MHC II as modified with branched Ub chains containing K11 and K63 Ub chain linkages.

Results

MARCH1 ubiquitinates I-A and I-E in cDCs and B cells

MHC II is a heterodimeric glycoprotein composed of two non-covalently linked polypeptide alpha (a) and beta (b) chains. We, and others, have previously shown K225 in the MHC IIb chain is the lysine modified by ubiquitination⁸. MHC II is encoded as diverse allotypes due to allelic polymorphism in the HLA locus. To investigate potential isotypic or allotypic differences in MHC II ubiquitination, MHC II was analysed in immune cells isolated from C57BL/6 and BALB/c mice that express different MHC II proteins. BALB/c mice express haplotype d of I-A (I-A^d) and I-E (I-E^d), while C57BL/6 mice express haplotype b of I-A (I-A^b), but do not express I-E¹⁹. We, and others have formally demonstrated MARCH1 ubiquitinates I-A^b, for example¹⁷, but have not investigated ubiquitination of other MHC II variants. To investigate if MARCH1 ubiquitinates both I-A^b and I-A^d haplotypes we measured MHC II at the surface of B cells from C57BL/6 (haplotype b) versus Balb/c (haplotype d) mice. Levels of MHC II at the cell surface can provide a surrogate read out for Ub-mediated plasma membrane trafficking whereby ubiquitinated MHC II is directed away from the plasma membrane with reduced cell surface expression. An inability to ubiquitinate MHC II elevates MHC II surface expression (for example¹⁷. Peripheral blood was isolated from C57BL/6, C57BL/6 × *Marchf1*^{-/-}, BALB/c and/or BALB/c × *Marchf1*^{-/-} and examined by flow cytometry. Increased MHC II was detected at the cell surface for BALB/c × *Marchf1*^{-/-} blood B cells, similar to that observed for C57BL/6 × *Marchf1*^{-/-} cells (Fig. 1A). This suggests MARCH1 ubiquitinates both b and d I-A haplotypes. Second, we investigated whether I-E is ubiquitinated, and whether this is mediated by MARCH1. The cytoplasmic tails of I-A and I-E vary in the flanking amino acids that surround the target K for ubiquitination²⁰ and this may alter MARCH1 recognition of I-A or I-E and/or dictate different configurations of attached Ub chains. To formally examine this, cDCs and B cells were enriched from spleen and MHC II immunoprecipitated using rabbit antisera specific for either I-A or I-E²¹. I-A was immunoprecipitated from C57BL/6 and BALB/c cells, while I-E was captured only from BALB/c cells. I-A immunoprecipitation revealed characteristic varying lengths of poly-Ub chains covalently attached to MHC II for both C57BL/6 and BALB/c cDCs and B cells. A poly-Ub chain was also evident for I-E immunoprecipitated from BALB/c cDCs and B cells indicating that MHC II I-E^d is also ubiquitinated (Fig. 1B, Supplementary Fig. 1). To demonstrate that MARCH1 is the E3 Ub ligase responsible for ubiquitination of I-E, MHC II was immunoprecipitated from splenic cDCs and B cells. *MHC II*^{-/-} cDCs were used as a negative control. For anti-I-A and I-E MHC II immunoprecipitates, Ub immunoblotting identified a poly-Ub chain in BALB/c cDCs and B cells that was absent in BALB/c × *Marchf1*^{-/-} cells (Fig. 1C, Supplementary Fig. 1). In summary, MARCH1 ubiquitinates MHC II I-A^b, I-A^d and I-E^d in cDCs and B cells.

UBE2D2/3, but not UBE2S or UBE2N E2 Ub ligases, regulates MHC II plasma membrane expression

We have previously identified that MARCH1 function relies on UBL3, an adaptor protein proposed to recruit E2 Ub ligases required for MARCH1-mediated MHC II ubiquitination²². The E2 Ub ligases themselves, however, are unknown. To assess E2 Ub ligases cooperating with MARCH1 to generate MHC II Ub chains, UBE2D2/3 and UBE2N, previously associated with viral MARCH homologues K3/K5^{23–25}, and UBE2S²⁶ were examined. Analysis was performed in Mutu DC cells²⁷ that regulate MHC II using MARCH1 ubiquitination similar to primary cDCs¹⁰. UBE2D2/3 and UBE2S E2 Ub ligases were targeted with siRNA, while UBE2N was deleted using CRISPR-Cas9. Depletion of UBE2S, UBE2D2 or UBE2D3 reduced respective protein levels by approximately 60–80%. Likewise, evaluation of four clonal cell lines expressing Cas9 and gRNA targeting *Ube2n* showed an approximately 60% reduction in UBE2N protein (Fig. 2A, Supplementary Fig. 2). Surface MHC II expression was examined by flow cytometry for the E2 Ub ligase depleted cells. We included a non-targeting siRNA or an siRNA targeting *Marchf1* as controls for unchanged or increased MHC II surface expression, respectively. We also examined the impact of E2 Ub ligase deletion on two other cell surface proteins; CD86, another known substrate of MARCH1 ubiquitination²², and MHC I, a protein that is not ubiquitinated by MARCH1¹⁰. Loss of UBE2D2/3 caused a significant increase in surface MHC II expression, albeit an increase that was smaller than that caused by the absence of MARCH1. This effect was specific to MHC II, as MHC I was not altered and no major change detected for CD86 (Fig. 2B). Deletion of UBE2S or UBE2N did not affect any of the surface proteins studied. To determine if UBE2D2/3 impacted MHC II ubiquitination, MHC II was immunoprecipitated from UBE2D2/3 or UBE2N-depleted cells. We found no significant change in MHC II ubiquitination in the absence of either UBE2D2/3 or UBE2N (Fig. 2C, Supplementary Fig. 2). Together, these results suggest that while UBE2D2/3 may impact MHC II surface turnover, this likely occurs through mechanisms independent of its role in direct MHC II ubiquitination.

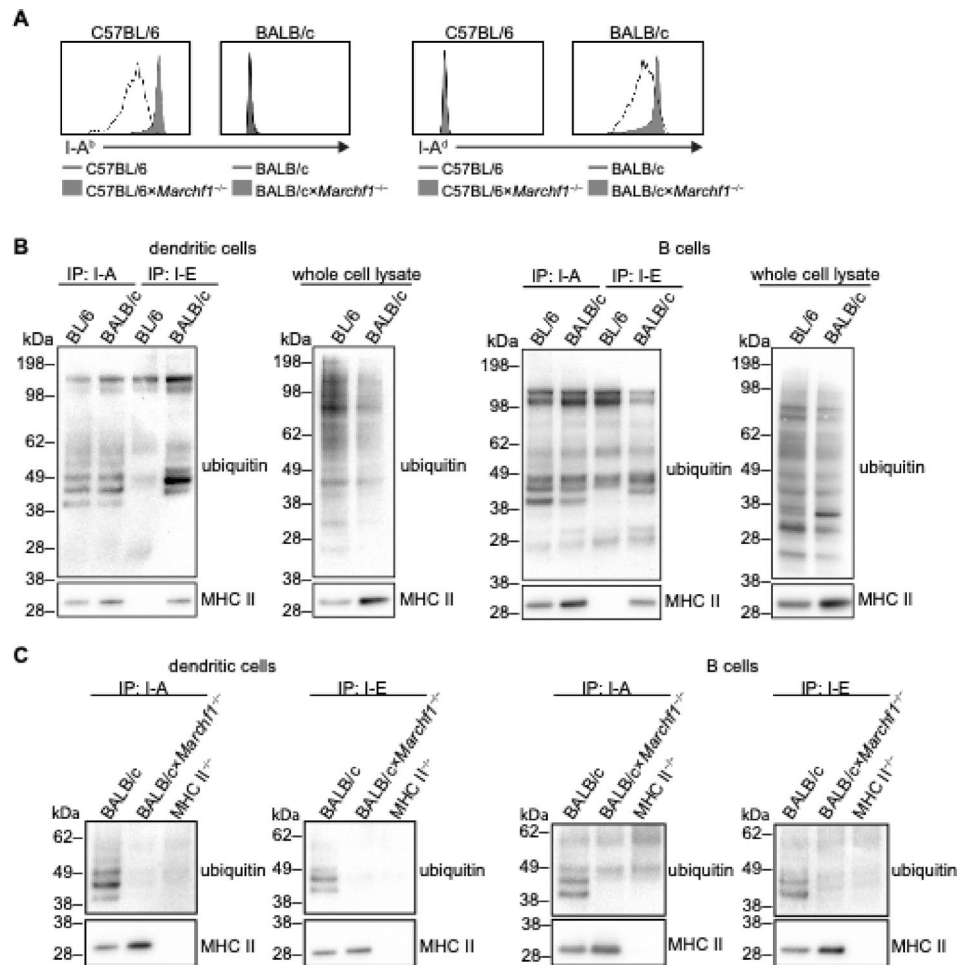


Fig. 1. MARCH1 ubiquitinates I-A and I-E in primary splenic cDCs and B cells. **(A)** Peripheral blood was isolated from C57BL/6, C57BL/6 × *March1*^{-/-}, BALB/c and/or BALB/c × *March1*^{-/-} and cells examined by flow cytometry. MHC II expression at the surface of B220⁺ B cells was determined by flow cytometry by staining cells with an antibody specific for I-A^b (clone 39-10-8) or I-A^d (clone AF6-120.1). **(B)** cDCs and B cells were enriched from spleens of C57BL/6 and BALB/c mice. Whole cell lysate was prepared and MHC II immunoprecipitated using rabbit antisera recognising I-A or I-E. Samples were denatured, analysed by SDS-PAGE and immunoblotting performed with antibodies specific for MHC II I-A/I-E (clone M5/114) or Ub (P4D1). Blots are representative of one (B cells) or two (cDCs) experiments. **(C)** Analysis of MHC II ubiquitination was undertaken as in (B) with splenic cDCs and B cells isolated from BALB/c, BALB/c × *March1*^{-/-} or *H2-Aa* (*MHC II*)^{-/-} mice. Blots are representative of 1–2 experiments.

MHC II I-A^b Ub chain in primary Splenic B cells and cDCs contains K11- and K63 Ub chain linkages

To characterise the poly-Ub chain associated with MHC II in B cells and cDCs, we first used the UbiCREST assay, where Ub chains associated with substrates are subjected to digestion by different Ub chain linkage-specific DUBs²⁸. In this assay the majority of ubiquitination was lost when MHC II, immunoprecipitated from cDCs, was incubated with AMSH which cleaves K63-linked Ub, or USP2 which cleaves all Ub chain linkages. In contrast, no changes in ubiquitination were detected after incubation with the K11-linked Ub specific DUB Cezanne or the K48-linked Ub specific DUB OTUB1 (Fig. 3A, **Supplementary Fig. 3**). This analysis identified the MHC II Ub chain generated by MARCH1 in cDCs and B cells as being composed of K63 Ub chain linkages.

Next, we performed Ub-Absolute QUAntification (Ub-AQUA) mass spectrometry, a more sensitive approach to determine the linkage composition of the poly-Ub chains associated with MHC II in B cells and cDCs. Trypsin digestion of poly-Ub chains generates signature peptides containing a di-glycine (GG) motif (Ub_{75–76}) present at the site of ubiquitination in the digested protein. Internal Ub lysines can also be assessed to enable mapping of the Ub chain linkages in a poly-Ub chain²⁹ (Fig. 3B). To characterize the MHC II-associated poly-Ub chain, I-A^b was immunoprecipitated from C57BL/6 primary splenic cDCs, digested with trypsin and mass spectrometry performed. Analysis identified 547 proteins with the three most abundant proteins being MHC II β-chain (H2-Ab1), MHC II α-chain (H2-Aa) and the MHC II chaperone, invariant chain (Cd74). Ub was the 5th most abundant protein (Fig. 3C). Several GG-modified Ub peptides identified corresponding to K11, K48 and K63 Ub chain linkages, in addition to unmodified Ub peptides (Table 1). The amount of specific Ub chain linkages

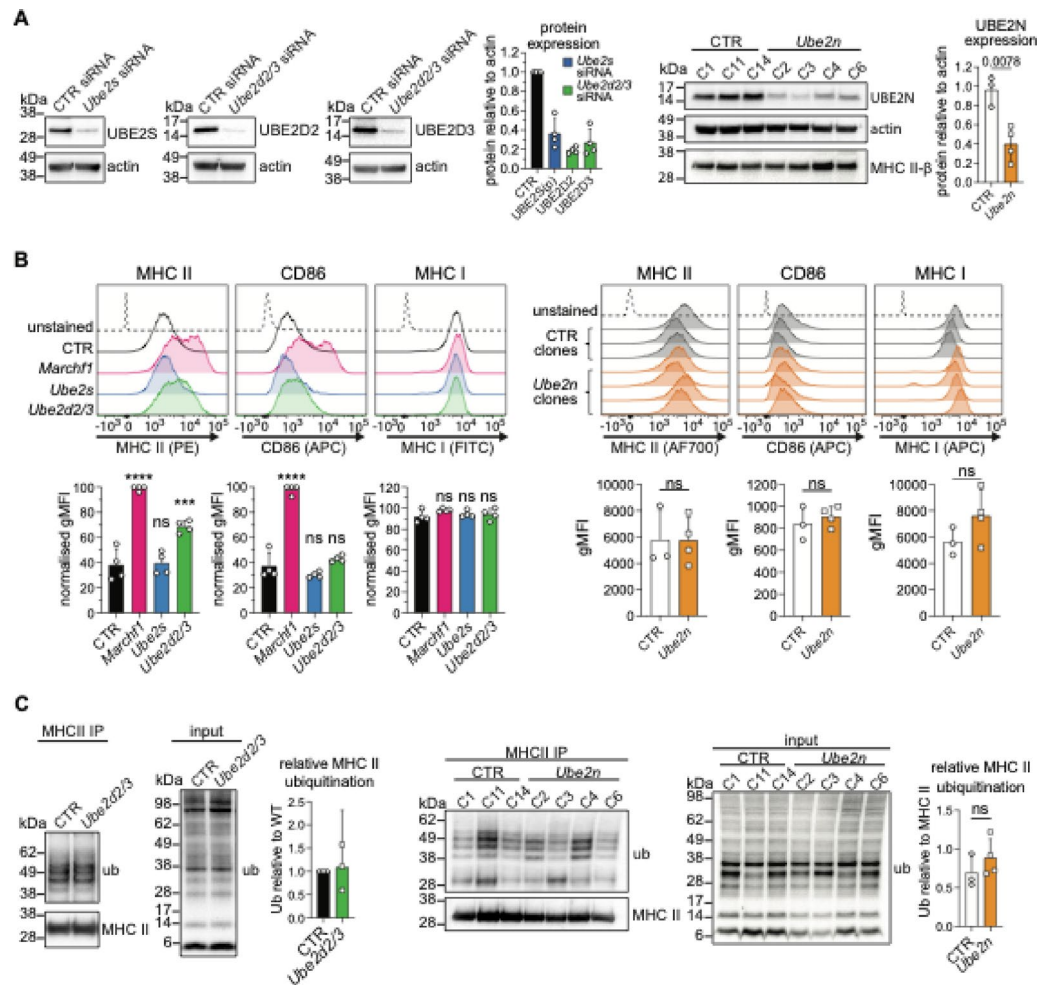


Fig. 2. UBE2D2/3, but not UBE2S or UBE2N E2 Ub ligases, regulates MHC II plasma membrane expression. (A–C) Mutu DCs were treated with non-targeting siRNA (CTR) or siRNA specific for *Ube2s* or *Ubed2d2/3*. Clonal Mutu DC knock out cell lines were generated expressing non-targeting sgRNA (CTR) or *Ube2n* sgRNA. (A) Cell lysates were analysed by SDS-PAGE followed by western transfer and UBE2S, UBE2D2, UBE2D3, UBE2N or actin detected by immunoblotting. Blots represent four independent siRNA experiments and one gRNA experiment. Protein expression was quantified by band densitometry, with siRNA graphs showing data pooled from four experiments with symbols representing independent replicates or, for gRNA graphs, showing pooled cell knock out clones. Bars indicate mean + 95%, Welch's t test, p-value as indicated. (B) Surface expression of MHC II, CD86 and MHC I was analysed by flow cytometry. *hBim*, a non-targeting gRNA (CTR), and *March1* siRNA were included as controls. Histograms are representative of four independent experiments. Left: graphs show gMFI normalised to highest value, with symbols representing independent replicates and bars mean + SD. **** $p < 0.0001$, *** $p < 0.001$, ns not significant, one-way ANOVA with Bonferroni's test. Right: graphs show gMFI from one experiment, with symbols representing individual clones and bars mean + SD. ns not significant, Welch's t test. (C) Cell lysates (input) or MHC II immunoprecipitates were analysed by SDS-PAGE and immunoblotting with antibodies for MHC II β -chain (JV2) or Ub (P4D1). Left: Blots are representative of three independent experiments. Relative ubiquitination compared to CTR was analysed by band densitometry in ImageJ, with symbols representing individual experiments, bars mean + 95% confidence interval. Right: Blot from one experiment, undertaken in duplicate. Symbols represent individual cell clones, bars mean + SD, ns not significant, Welch's t test.

was determined using AQUA (absolute quantification) for MHC II immunoprecipitated from C57BL/6 mice (WT) or *Marchf1*^{-/-} primary cDCs or B cells (**Supplementary Fig. 4**). *Marchf1*^{-/-} cells were included to control for the presence of other ubiquitinated proteins that may also be present in the MHC II immunoprecipitates. For I-A^b isolated from cDCs, K63 and K11 Ub chain linkages were significantly increased in WT versus *Marchf1*^{-/-} controls. A small amount of K48 Ub chain linkages was detected, but this was unaltered by the absence of MARCH1. A similar pattern of markedly increased K63 and K11 Ub chain linkages were detected in WT, as compared to *Marchf1*^{-/-} B cells (Fig. 3D). Together, this suggested that MHC II in primary splenic cDCs and B cells is associated with a poly-Ub chain composed of K63 and K11 Ub chain linkages.

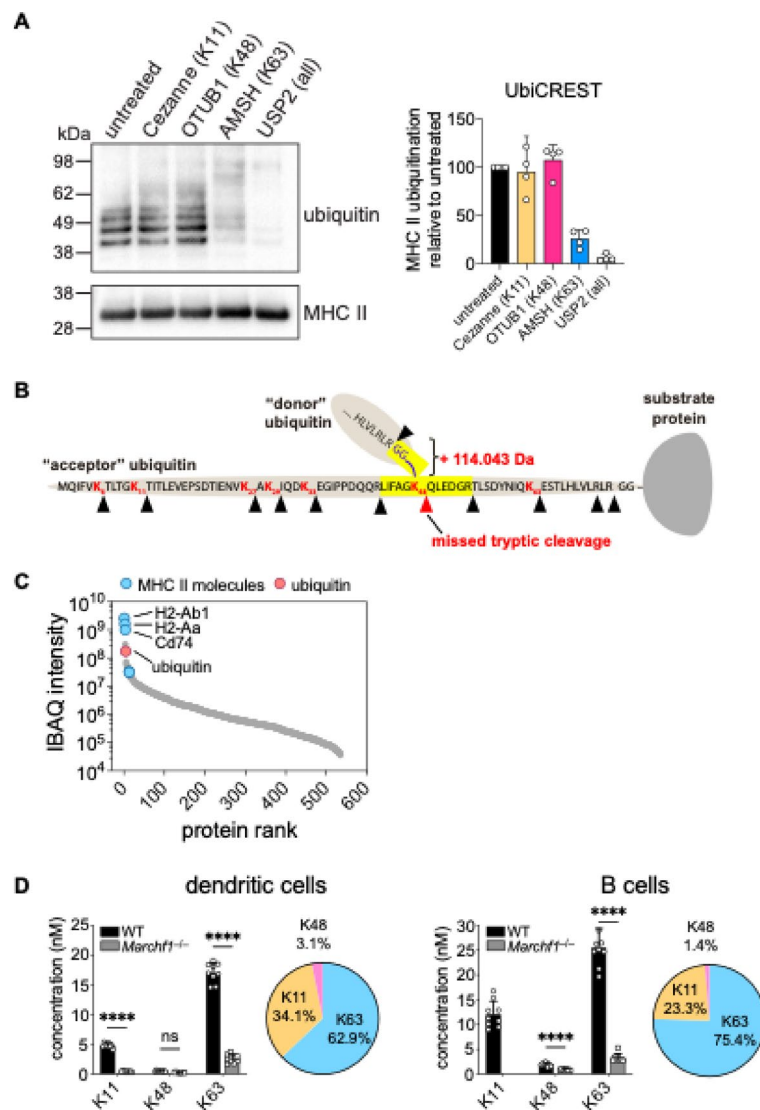


Fig. 3. MHC II I-A^b in primary splenic cDCs and B cells is modified with K11 and K63-linked poly-Ub chains. **(A)** UbiCREST was undertaken using MHC II immunoprecipitated from spleen cDCs enriched from C57BL/6 mice. MHC II immunoprecipitates were treated with DUBs specific for K11 (Cezanne), K48 (OTUD1) or K63 (AMSH)-linked Ub chains, as well as unspecific USP2. Samples were analysed by SDS-PAGE, western and immunoblotting for Ub (P4D1) or MHC II β -chain (JV2). Blot is representative of four independent experiments. Relative ubiquitination compared to untreated sample was quantified by densitometry in ImageJ, with symbols representing individual experiments, bar is mean + 95% CI. **(B)** Schematic of Ub linkage analysis. Proximal Ub shown with all internal lysines (in red) and all possible tryptic cleavage sites (black arrowheads). A second Ub is bound to the proximal Ub at K48. The predicted signature peptide is highlighted in yellow, including the GG remnant of Ub_{75–76}, and a missed tryptic cleavage (red arrowhead). **(C)** MHC II was immunoprecipitated from splenic cDCs enriched from C57BL/6 mice. Eluates were digested with trypsin and analysed by mass spectrometry. **(D)** MHC II was immunoprecipitated from splenic cDCs or B cells from C57BL/6 or *Marchf1*^{-/-} mice. Eluates were digested with trypsin and analysed by mass spectrometry using Absolute QUAntification (AQUA methodology). Bars represent mean + SD. Each graph shows one experiment with three biological and three technical replicates. Statistical analysis was undertaken using a two-way ANOVA with Bonferroni's multiple comparisons test, comparing WT with *Marchf1*^{-/-} for each Ub chain linkage type. *****p* < 0.0001, ns not significant.

1 MHC II was immunoprecipitated from splenic cDCs enriched from C57BL/6 mice. Eluates were digested with trypsin and analysed by mass spectrometry.

MHC II I-A^b in primary cDCs is modified with branched Ub chains

As previously highlighted, ubiquitination of MHC II I-A β -chain occurs at a single lysine (K225)^{30,31}. Since multiple Ub chain linkage types were detected in our analysis this indicated either a mixed linear or branched Ub chain architecture (Fig. 4A). To determine the poly-Ub architecture and possible presence of branching we

Sequence	Charge	m/z	Mass	Predicted Gly-Gly location in peptide	Predicted (Lys) Ub chain linkage
ESTLHLVLR	2	534.31402	1066.613		
ESTLHLVLR	3	356.54510	1066.613		
LIFAGKQLEDGR	3	487.60005	1459.778	LIFAGK(1)QLEDGR	K48
TITLEVEPSDTIENVK	2	894.46728	1786.920		
TITLEVEPSDTIENVK	3	596.64728	1786.920		
TLSDYNIQK	2	541.27984	1080.545		
TLSDYNIQKESTLHLVLR	4	561.80502	2243.191	TLSDYNIQK(1)ESTLHLVLR	K63
TLTGKTITLEVEPSDTIENVK	3	801.42687	2401.259	TLTGK(1)TITLEVEPSDTIENVK	K11

Table 1. MHC II-associated Ub peptides detected by mass spectrometry.

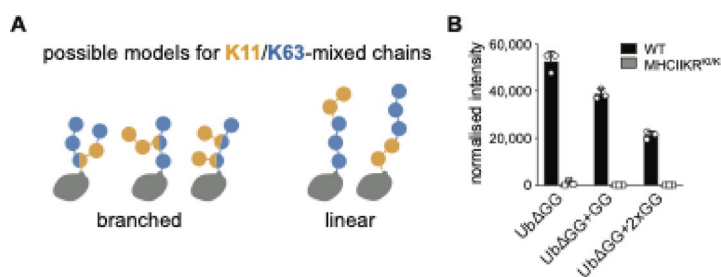


Fig. 4. MHC II in primary splenic cDCs is modified with branched Ub chains. (A) Schematic of possible K11 and K63-linked Ub chain architectures. (B) MHC II immunoprecipitated from spleen cDCs of C57BL/6 or MHC II K225R^{K1/K1} mice was treated with Lb^{Pro*} and the relative abundance of different Ub species: “endcap” (UbΔGG) (8,451.65 Da), “linear chain” (UbΔGG + 1xGG) (8,565.69 Da) and “branched chain” (UbΔGG + 2xGG) (8,679.73 Da) quantified by intact mass spectrometry. Symbols show biological replicates, with bars mean + SD.

used an engineered viral protease Lb^{Pro*} that cleaves poly-Ub chains into “clipped” Ub monomers (UbΔGG) leaving a signature GG motif on the substrate, resulting in “endcap” (UbΔGG), “linear chain” (UbΔGG + 1xGG) and “branched chain” (UbΔGG + 2xGG). This approach enables Ub chain architecture to be determined by intact mass spectrometry. Primary spleen cDCs were isolated from WT or MHC II K225R^{K1/K1} mice, that lack the acceptor lysine for ubiquitination¹². I-A^b was immunoprecipitated and treated with Lb^{Pro*}. Intact mass spectrometry detected Ub species corresponding to 46.7% (± 1.2%) “endcap”, 34.4% (± 1.2%) “linear chain” and 18.9% (± 0.3%) “branched chain” Ub units associated with WT MHC II. As expected very little Ub was detected for MHC II K225R^{K1/K1} cells (Fig. 4B). This indicated the presence of branching in the MHC II poly-Ub chain. Altogether, we concluded the MHC II Ub chain in cDCs contained branches of K11 and K63-linked Ub chains.

Discussion

MHC II ubiquitination by MARCH E3 Ub ligases is a fundamental mechanism of MHC II regulation in both mouse and human cells. It plays critical roles in both adaptive and innate immune responses⁴. Here, for the first time, we provide novel and significant insights into the composition and architecture of the MHC II Ub chain and provide the first description of a Ub chain generated by MARCH 1, an E3 Ub ligase of significant interest in health and disease, for a transmembrane substrate in primary cells.

We, and others, have formally demonstrated MHC II I-A ubiquitination by MARCH1⁴ and we now extend this to MHC II I-E in primary mouse splenic cDCs and B cells. Previous reports have highlighted that the poly-Ub chain associated with MHC II in B cells is shorter in Ub units than in cDCs³². Given that MARCH 1 is the responsible E3 Ub ligase in both cell types²², it is likely that the MHC II Ub chain is modified by cell-specific Ub machinery e.g. an E2 ligase or DUB. Our analysis here of a selected panel of E2 Ub ligases did not identify a conclusive E2 Ub ligase participant in MARCH1-mediated MHC II ubiquitination. These experiments were limited by the difficulty in deleting E2 Ub ligases, where many of which can play multiple roles in cell function and are often essential for cell survival. Our analysis identified that UBE2D2/3 participates in regulating MHC II plasma membrane expression, but we could not detect UBE2D2/3 directly mediating MHC II ubiquitination. This discrepancy may be due to UBE2D2/3 regulating MHC II surface expression via an indirect mechanism independent of MHC II ubiquitination. This highlights the complexity of E2 Ub ligase analysis and the importance of directly examining the ubiquitination status of substrates where possible. Further analysis could attempt to examine a broader array and/or combination of multiple E2 Ub ligases given that it is possible that multiple E2 Ub ligases play redundant roles in the generation of Ub chains.

Several parameters of a poly-Ub chains encode instructions regarding the substrate protein. These include the number of Ub monomers, types of Ub chain linkages and the overall topology (e.g. linear, branched chains). For MHC II, the length of the MHC II-associated poly-Ub chain had previously been described for primary

cells³³, and a study has reported that mature MHC II in the MelJuso melanoma cell line is associated with K11, K33, K48 and K63-linked Ub chains³⁴. Our data identifies that in primary splenic cDCs and B cells, MHC II-associated poly-Ub chains consist of K11 and K63-linked Ub, in which 19% of Ub moieties are present in “forks” containing K11 and K63-linked branched Ub chains. This conclusion is based on our analyses using both trypsin-digested and intact mass spectrometry, together with DUB-based methodologies. Identification of a branched Ub chain associated with MHC II is highly novel, with the identification of branched Ub chains to date having been described for very few proteins. This is one of the few examples of branched Ub chains participating in the endocytosis of cell surface receptors. Moreover, it is the first description of the features of the Ub chain generated by MARCH E3 Ub ligases in primary cells, E3 Ub ligases that are highly specialized in the ubiquitination of membrane associated proteins.

Our findings for the MHC II poly-Ub chain concur with observations of K11 and K63-linked mixed Ub chains associated with the closely related MHC I protein in cells where the viral MARCH homologue K5 is overexpressed²⁵. It is unknown in this case whether this Ub chain is branched. How do K11 and K63-linked branched Ub chains signal a different fate than homotypic K63-linked chains alone? Knowledge to date suggests that branched heterotypic poly-Ub chains function by enhancing existing Ub signals. During mitosis, K11 and K48-branched Ub chains increased substrate affinity to the proteasome compared to K11 or K48-linked Ub chains alone³⁵. Assembly of K48 and K63-linked Ub chains were proposed to protect the Ub chain from cleavage by K63-specific DUBs and as a result lead to sustained signaling³⁶. For K11 and K63-linked Ub chains associated with MHC II, evidence based on MHC I-ubiquitination by viral E3 Ub ligases suggests a scenario where while K11 or K63 Ub chains alone can be sufficient to induce MHC I internalization and downregulation, the presence of both increases the efficiency of this process²⁵. The exact mechanism by which MHC II-associated branched K11 and K63-linked Ub chain functions remains to be elucidated, whether through blocking of a specific DUB or altering affinity towards an internalization, sorting or signaling adaptor e.g. UBL3²².

In summary, our findings provide the first description of MHC II poly-Ub chain architecture in primary antigen presenting cells. This information provides critical insight into understanding MHC II turnover and function and the mechanisms of MARCH E3 Ub ligase-mediated regulation of transmembrane proteins.

Materials and methods

Mice

C57BL/6 (H-2^b) (bred in house), BALB/c (H-2^d) (sourced from Walter and Eliza Hall Institute, Australia), C57BL/6 × *Marchf1*^{-/-37} (sourced as a gift from Satoshi Ishido, Hyogo Medical University, Japan), BALB/c × *Marchf1*^{-/-}, *H2-Aa*^{-/-} mice (sourced from Walter and Eliza Hall Institute, Australia)³⁸ and MHC II K225R^{K1/K1} mice (sourced as a gift from Satoshi Ishido, Hyogo Medical University, Japan)¹² were used at 6–12 weeks of age. All mice were bred and maintained in specific pathogen free conditions at the Melbourne Bioresources Platform at Bio21 Molecular Science and Biotechnology Institute. Mice were euthanized by carbon dioxide asphyxiation with a flow rate of 50% volume per chamber size per minute followed by cervical dislocation. Experimental procedures were approved by the Animal Ethics Committee of the University of Melbourne. All methods were carried out according with the relevant guidelines and regulations. All methods are reported in accordance with ARRIVE guidelines.

Isolation of primary immune cells

Spleens were digested with DNase I (Roche) and collagenase type 3 (Worthington Biochemicals) and light density cells collected after density gradient separation in 1.077 g/cm³ Nycodenz (Nycomed Pharma). cDCs were further enriched by a depletion cocktail containing rat anti-mouse mAbs specific for CD3 (KT3-1.1), Thy1 (T24/31.7), red blood cells (Ter119), B220 (RA3-6B2), and Ly6c/g (RB6-8C5) (all Walter and Eliza Hall Antibody facility) and magnetic separation with BioMag anti-rat IgG-coupled magnetic beads (Qiagen). This protocol typically generates 70–90% CD11c⁺ DC purity, with < 5% MHC II expressed on non-CD11c⁺ cells as determined by flow cytometry. To enrich B cells, spleens were dissociated using manual disruption with a 40 µm cell strainer (Falcon). Light density cells were enriched using centrifugation over a Ficoll-paque (GE Healthcare). This protocol typically generates 60–70% B220⁺ cell purity, with < 5% of MHC II expressing cells B220⁻ as determined by flow cytometry. Flow cytometry gating strategies were used as described previously²².

Cell lines

Mutu DCs were a gift from Hans Acha-Orbea³². To generate UBE2N haploinsufficient cells, Mutu DCs were lentivirally transduced with FUCas9Cherry (Addgene plasmid # 70182, gifted by Marco Herold) and mCherry⁺ cells sorted by flow cytometry. Specific gRNAs were designed using the Broad Institute GPP sgRNA Designer³⁹ and cloned into the dox-inducible FgH1t_UTG vector (Addgene plasmid #70183, a gift from Marco Herold), with gRNA sequences: *Ube2n* exon 2: 5' TAACGGGCGTTGCTCTCATC 3'; *hBIM* exon 3: 5' GCCCAAGA GTTGCGGCGTAT 3'. Lentivirally transduced cells were treated with 1 µg/mL doxycycline (Sigma-Aldrich) for 3 days to induce gRNA transcription, and single CFP⁺ cells were sorted using a Beckton Dickinson Influx cell sorter (BD Biosciences). Target editing of clonal cell lines was assessed using Sanger sequencing and ICE CRSIPR Analysis Tool⁴⁰. Sequencing analysis is provided in **Supplementary Fig. 5**.

E2 Ub ligase siRNA knockdown and knockout analysis

Mutu DCs were seeded at 600,000 cells per well in six-well plates and reverse-transfected with 50 nM siRNA against *Marchf1* (s91382), *Ube2s* (s95262 + s95264) or *Ubed2d2/3* (s234443) using Lipofectamine RNAiMAX (all Thermo Fisher). After 48 h, cells were harvested, washed and analysed by western blot or flow cytometry. To confirm E2 Ub ligase knockdown, cells were lysed in non-reducing lysis buffer, separated on 4–12% NuPage gels, transferred to PVDF (all Thermo Fisher), and incubated with primary antibodies against UBE2D2,

UBE2D3, UBE2S or UBE2N overnight at 4 °C, followed by incubation with horse radish peroxidase conjugated anti-rabbit secondary antibody (all Cell Signaling Technologies). Loading control was detected using β -actin. Chemiluminescence was detected using ECL select substrate (GE Healthcare) and ChemiDoc MP imaging (Bio-Rad) and analysed in ImageJ.

Flow cytometry

Cells were stained with mAbs specific for B220 (RA3-6B2), CD11c (N418), CD86 (clone GL1, BioLegend), MHC I (Y3), MHC II pan I-A/I-E (M5/114), MHC II IAb^{b8,10,39} and MHC II IA^d (AF6-120.1) (Walter and Eliza Hall Institute Antibody facility). Cells were analysed using a LSRFortessa (BD Biosciences). Data was analyzed with FlowJo v10 (Tree Star) and statistical analysis performed with Prism v9 (Graphpad).

MHC II immunoprecipitation

Cells were lysed in 20 mM Tris pH 7.5, 150 mM NaCl, 1 mM EDTA, 1% v/v Triton X-100, 10 mM N-ethylmaleimide, complete protease inhibitor cocktail (Roche) and nuclei removed by centrifugation at 14,000 g. MHC II was immunoprecipitated with protein-G sepharose conjugated with mAb to pan-MHC II mAb (clone M5/114) or rabbit antisera specific for I-A α -chain (JV1) or I-E α -chain (JV3). For western blot analysis horseradish peroxidase (HRP)-conjugated anti-Ub mAb P4D1 (Santa Cruz) or rabbit polyclonal serum generated against I-A β -chain (JV2), followed by HRP-coupled donkey anti-rabbit IgG (Cell Signaling Technology) were used to detect Ub and MHC II, respectively.

UbiCrest assay of Ub chain linkages

MHC II immunoprecipitates were incubated in the presence of Cezanne, OTUD1, AMSH and USP2 (R&D Systems) at 37 °C for 30 min. Samples were denatured and analysed by SDS-PAGE and immunoblotting for Ub (P4D1) or MHC II β -chain (JV2). Relative ubiquitination compared to untreated sample was quantified by densitometry in ImageJ.

Ub chain linkage analysis by trypsin digestion and mass spectrometry

MHC II immunoprecipitates from splenic cDCs and B cells and heavy-labelled Ub peptide standards (SpikeTides TQL, JPT Peptide Technologies, Germany) were prepared for mass spectrometry using the FASP protein digestion method as previously described⁴¹ with the following modifications. Protein was reduced with Tris-(2-carboxyethyl) phosphine (TCEP, 10 mM final concentration) and digested with 1 μ g sequence-grade modified Trypsin Gold (Promega). Peptides were eluted with 50 mM ammonium bicarbonate and acidified in 1% formic acid. Peptides were lyophilized, reconstituted and separated by reverse-phase chromatography on a 1.9 μ m C18 fused silica column (I.D. 75 μ m, O.D. 360 μ m x 25 cm length) packed into an emitter tip (Ion Opticks, Australia), using a nano-flow HPLC (M-class, Waters). The HPLC was coupled to an Impact II UHR-QqTOF mass spectrometer (Bruker, Bremen, Germany) using a CaptiveSpray source and nanoBooster at 0.20 Bar using acetonitrile. Mass spectrometry spectra were acquired between a mass range of 200–2000 m/z. Peptide fragmentation was performed using collision-induced dissociation. For label-free quantification of protein abundance, mass-adjusted intensities were estimated using the iBAQ (intensity based absolute quantification) algorithm⁴². For AQUA analysis, calibration curves were created using heavy-labelled Ub peptide (K11, K48, K63) SpikeTides™ TQL (JPT Peptide Technologies) (**Supplementary Fig. 4**). Raw mass spectrometry data were imported into and analysed using Skyline v.4.1.0 where MS1 precursor scans were extracted from data dependent acquisition experiments⁴³. Peak areas for precursor masses were integrated across all precursor isotope ions for each sample replicate. Calibration curves were created based on peak area abundances for heavy-labelled peptide standards to measure absolute abundances of endogenous K11, K48 and K63 Ub peptides within each immunoprecipitate based on integrated peak areas. Mass spectrometry proteomics data has been deposited to the ProteomeXchange Consortium via the PRIDE⁴⁴ partner repository with the dataset identifier PXD063057.

Analysis of poly-Ub chain branching by mass spectrometry

MHC II was immunoprecipitated from splenic cDCs and MHC II was Ub-clipped as described by Swatek et al. (2019). Briefly, Lb^{PRO*} clipping was performed on MHC II immunoprecipitated eluates followed by ammonium sulfate precipitation. Samples were centrifuged at 21,000 g and the soluble fraction, containing the clipped mono Ub, was retained. The supernatant was desalted using a 3 kDa molecular weight cutoff column (Amicon). Lb^{PRO*}-treated samples were dried and resuspended in 50% acetonitrile (v/v), 0.1% formic acid (v/v). Samples were directly infused onto a MaXis II mass spectrometer (Bruker) at 5 μ l min⁻¹. Spectra were averaged and deconvoluted using the Maximum Entropy algorithm in the Data Analysis software package (Bruker).

The intensities of “endcap” (Ub Δ GG) (8,451.65 Da), “linear chain” (Ub Δ GG + 1xGG) (8,565.69 Da), and “branched chain” (Ub Δ GG + 2xGG) (8,679.73 Da) Ub were exported into Microsoft Excel for further analysis.

Data availability

Mass spectrometry proteomics data has been deposited to the ProteomeXchange Consortium via the PRIDE partner repository with the dataset identifier PXD063057.

Received: 28 May 2025; Accepted: 24 October 2025

Published online: 25 November 2025

References

1. Komander, D. & Rape, M. The Ubiquitin Code. in *Annual Review of Biochemistry*, pp 203–229. (2012).

2. Haakonsen, D. L. & Rape, M. Branching out: improved signaling by heterotypic ubiquitin chains. *Trends Cell. Biol.* **29**, 704–716 (2019).
3. French, M. E., Koehler, C. F. & Hunter, T. Emerging functions of branched ubiquitin chains. *Cell. Discov.* **7**, 6 (2021).
4. Liu, H., Mintern, J. D. & Villadangos, J. A. MARCH ligases in immunity. *Curr. Opin. Immunol.* **58**, 38–43 (2019).
5. Liu, H. et al. Ubiquitin ligase MARCH 8 cooperates with CD83 to control surface MHC II expression in thymic epithelium and CD4 T cell selection. *J. Exp. Med.* **213**, 1695–1703 (2016).
6. von Rohrscheidt, J. et al. Thymic CD4 T cell selection requires Attenuation of March8-mediated MHCII turnover in cortical epithelial cells through CD83. *J. Exp. Med.* **213**, 1685–1694 (2016).
7. Schriek, P. et al. Marginal zone B cells acquire dendritic cell functions by trogocytosis. *Science* **375**, eabf7470 (2022).
8. Bandola-Simon, J. & Roche, P. A. Regulation of MHC class II and CD86 expression by March-I in immunity and disease. *Curr. Opin. Immunol.* **82**, 102325 (2023).
9. Bannard, O. et al. Ubiquitin-mediated fluctuations in MHC class II facilitate efficient germinal center B cell responses. *J. Exp. Med.* **213**, 993–1009 (2016).
10. Wilson, K. R. et al. MARCH1-mediated ubiquitination of MHC II impacts the MHC I antigen presentation pathway. *PLoS One.* **13**, e0200540–e0200540 (2018).
11. Wilson, K. R. et al. MHC class II ubiquitination regulates dendritic cell function and immunity. *J. Immunol.* **207**, 2255–2264 (2021).
12. Walseng, E. et al. Ubiquitination regulates MHC class II-peptide complex retention and degradation in dendritic cells. *Proc. Natl. Acad. Sci.* **107**, 20465–20470 (2010).
13. Cho, K. J., Walseng, E., Ishido, S. & Roche, P. A. Ubiquitination by March-I prevents MHC class II recycling and promotes MHC class II turnover in antigen-presenting cells. *Proc. Natl. Acad. Sci. U S A.* **112**, 10449–10454 (2015).
14. Ohmura-Hoshino, M. et al. Requirement of MARCH-I-Mediated MHC II ubiquitination for the maintenance of conventional dendritic cells. *J. Immunol.* **183**, 6893–6897 (2009).
15. Kim, H. J. et al. Ubiquitination of MHC class II by March-I regulates dendritic cell fitness. *J. Immunol.* **206**, 494–504 (2021).
16. Oh, J. et al. MARCH1-mediated MHCII ubiquitination promotes dendritic cell selection of natural regulatory T cells. *J. Exp. Med.* **210**, 1069–1077 (2013).
17. Liu, H. et al. Ubiquitination of MHC class II is required for development of regulatory but not conventional CD4(+) T cells. *J. Immunol.* **205**, 1207–1216 (2020).
18. Ishikawa, R., Kajikawa, M. & Ishido, S. Loss of MHC II ubiquitination inhibits the activation and differentiation of CD4 T cells. *Int. Immunol.* **26**, 283–289 (2014).
19. Mathis, D. J., Benoist, C., Williams, V. E. 2, Kanter, M., McDevitt, H. O. & nd, Several mechanisms can account for defective E alpha gene expression in different mouse haplotypes. *Proc. Natl. Acad. Sci. U S A.* **80**, 273–277 (1983).
20. Harton, J., Jin, L., Hahn, A. & Drake, J. Immunological Functions of the Membrane Proximal Region of MHC Class II Molecules. *F1000Res* **5** (2016).
21. Villadangos, J. A., Riese, R. J., Peters, C., Chapman, H. A. & Ploegh, H. L. Degradation of mouse invariant chain: roles of cathepsins S and D and the influence of major histocompatibility complex polymorphism. *J. Exp. Med.* **186**, 549–560 (1997).
22. Liu, H. et al. Ubiquitin-like protein 3 (UBL3) is required for MARCH ubiquitination of major histocompatibility complex class II and CD86. *Nat. Commun.* **13**, 1934 (2022).
23. Dodd, R. B. et al. Solution structure of the kaposi's sarcoma-associated herpesvirus K3 N-terminal domain reveals a novel E2-binding C4HC3-type RING domain. *J. Biol. Chem.* **279**, 53840–53847 (2004).
24. Duncan, L. M. et al. Lysine-63-linked ubiquitination is required for endolysosomal degradation of class I molecules. *EMBO J.* **25**, 1635–1645 (2006).
25. Boname, J. M. et al. Efficient internalization of MHC I requires lysine-11 and lysine-63 mixed linkage Polyubiquitin chains. *Traffic* **11**, 210–220 (2010).
26. Katherine, E. et al. The Mechanism of Linkage-Specific Ubiquitin Chain Elongation by a Single-Subunit E2. *Cell* **144**, 769–781 (2011).
27. Steiner, Q. G. et al. In vivo transformation of mouse conventional CD8a+ dendritic cells leads to progressive multisystem histiocytosis. *Blood* **111**, 2073–2082 (2008).
28. Hospenthal, M. K., Mevissen, T. E. T. & Komander, D. Deubiquitinase-based analysis of ubiquitin chain architecture using ubiquitin chain restriction (UbiCRest). *Nat. Protoc.* **10**, 349–361 (2015).
29. Kirkpatrick, D. S. et al. Quantitative analysis of in vitro ubiquitinated Cyclin B1 reveals complex chain topology. *Nat. Cell Biol.* **8**, 700–710 (2006).
30. Shin, J. S. et al. Surface expression of MHC class II in dendritic cells is controlled by regulated ubiquitination. *Nature* **444**, 115–118 (2006).
31. van Niel, G. et al. Dendritic cells regulate exposure of MHC class II at their plasma membrane by oligoubiquitination. *Immunity* **25**, 885–894 (2006).
32. Fuertes Marraco, S. A. et al. Novel murine dendritic cell lines: a powerful auxiliary tool for dendritic cell research. *Front. Immunol.* **3**, 331–331 (2012).
33. Ma, J. K., Platt, M. Y., Eastham-Anderson, J., Shin, J. S. & Mellman, I. MHC class II distribution in dendritic cells and B cells is determined by ubiquitin chain length. *Proc. Natl. Acad. Sci.* **109**, 8820–8827 (2012).
34. Alix, E. et al. The tumour suppressor TMEM127 is a Nedd4-Family E3 ligase adaptor required by Salmonella to ubiquitinate and degrade MHC class II molecules. *Cell. Host Microbe.* **28**, 54–68 (2020). e57.
35. Meyer, H. J. & Rape, M. Enhanced protein degradation by branched ubiquitin chains. *Cell* **157**, 910–921 (2014).
36. Ohtake, F., Saeki, Y., Ishido, S., Kanno, J. & Tanaka, K. The K48-K63 branched ubiquitin chain regulates NF-kappaB signaling. *Mol. Cell.* **64**, 251–266 (2016).
37. Matsuki, Y. et al. Novel regulation of MHC class II function in B cells. *EMBO J.* **26**, 846–854 (2007).
38. Kontgen, F., Suss, G., Stewart, C., Steinmetz, M. & Bluethmann, H. Targeted disruption of the MHC class II Aa gene in C57BL/6 mice. *Int. Immunol.* **5**, 957–964 (1993).
39. Doench, J. G. et al. Optimized SgRNA design to maximize activity and minimize off-target effects of CRISPR-Cas9. *Nat. Biotechnol.* **34**, 184–191 (2016).
40. Brinkman, E. K., Chen, T., Amendola, M. & van Steensel, B. Easy quantitative assessment of genome editing by sequence trace decomposition. *Nucleic Acids Res.* **42**, e168 (2014).
41. Wisniewski, J. R., Zougman, A., Nagaraj, N. & Mann, M. Universal sample Preparation method for proteome analysis. *Nat. Methods.* **6**, 359–362 (2009).
42. Schwanhausser, B. et al. Global quantification of mammalian gene expression control. *Nature* **473**, 337–342 (2011).
43. Schilling, B. et al. Platform-independent and label-free quantitation of proteomic data using MS1 extracted ion chromatograms in skyline: application to protein acetylation and phosphorylation. *Mol. Cell. Proteom.* **11**, 202–214 (2012).
44. Perez-Riverol, Y. et al. The PRIDE database at 20 years: 2025 update. *Nucleic Acids Res.* **53**, D543–D553 (2025).

Acknowledgements

JDM acknowledges funding from National Health and Medical Research Council, Australia Project Grant

APP1161101. JAV acknowledges funding from Australian Research Council Discovery Project DP110101383 and DP160103134; from National Health and Medical Research Council, Australia Program Grant 1016629, 1123293 and Fellowship 1058193 and 1154502. JAV acknowledges funding from Human Frontiers Science Program grant 0064/2011.

Author contributions

J.M. and H.L. wrote the manuscript. J.M. and J.A.V. designed and managed the study. H.L., L.F., S.C. and L.D. conducted experiments. A.W. provided experimental advice and expertise. D.K. provided experimental advice and reagents.

Declarations

Competing interests

The authors declare no competing interests.

Additional information

Supplementary Information The online version contains supplementary material available at <https://doi.org/10.1038/s41598-025-25817-4>.

Correspondence and requests for materials should be addressed to J.A.V. or J.D.M.

Reprints and permissions information is available at www.nature.com/reprints.

Publisher's note Springer Nature remains neutral with regard to jurisdictional claims in published maps and institutional affiliations.

Open Access This article is licensed under a Creative Commons Attribution-NonCommercial-NoDerivatives 4.0 International License, which permits any non-commercial use, sharing, distribution and reproduction in any medium or format, as long as you give appropriate credit to the original author(s) and the source, provide a link to the Creative Commons licence, and indicate if you modified the licensed material. You do not have permission under this licence to share adapted material derived from this article or parts of it. The images or other third party material in this article are included in the article's Creative Commons licence, unless indicated otherwise in a credit line to the material. If material is not included in the article's Creative Commons licence and your intended use is not permitted by statutory regulation or exceeds the permitted use, you will need to obtain permission directly from the copyright holder. To view a copy of this licence, visit <http://creativecommons.org/licenses/by-nc-nd/4.0/>.

© The Author(s) 2025